Iranian Int. J. Sci. ***5****(2), 2004, p.203-221*

Petrophysical Evaluation and Determination of Rock Types in a Carbonate Reservoir in SW Iran with Interpretation of Petrography and Geophysical Well Logs

Beiranvand, B., Kamali, M.R.
Research Institute of Petroleum Industry-NIOC
(received: 20/10/2003 ; accepted: 5/1/2004)

Abstract

Reservoir characterization plays a critical role in appraising the economic success of reservoir management and development methods. This study identifies the different rock types that comprise reservoirs, marginal reservoirs and non-reservoirs. Porosity and permeability are the key parameters for identifying the rock types and reservoir characterization. The qualification of these parameters is usually measured directly from cores using conventional core analysis methods, and indirectly using geophysical well logs, well tests, and artificial neural network methods. However, for determination of rock types and reservoir evaluation, in addition to quantity of porosity and permeability we need to determine pore geometry and pore aperture size which are related to grain size, sorting and packing as well as to factors such as the mineralogy and diagenetic history of the reservoir.

This paper presents the results of a combination of conventional core analysis, capillary pressure curve characteristics, compressional net stress analysis, thin sections and SEM petrographical investigations integrated with geophysical well logs. A total of 4 different rock types were identified within the reservoir interval, in addition to two types of pore throat, one with a larger flow capacity than the other. The low permeability in non-reservoir rock types is probably related to higher amounts of clay minerals that affect pore throat connectivity and fining the pore throats between the microcrystalline calcites in the reservoir.

Keywords: *Petrophysics, Rock Types, Carbonate Reservoir, Iran.*

Introduction

Identification of rock types and their most significant vertical and lateral heterogeneities, is a primary goal of the reservoir characterization process, by incorporating this information into a three-dimensional geological and flow simulation models. The reservoir characterization process integrates multiple data sets to provide a description of the static and dynamic properties of a reservoir; especially those that control fluid flow.

Characterization of porosity and permeability of the reservoir is the focus of this paper. Pore scale heterogeneity in carbonates has long been identified as an important control on reservoir productivity. Petrophysicists, reservoir engineers and reservoir geologists must obtain porosity and permeability data to be able to predict fluid migration pathways and volumes. For determination and estimation of these parameters there are several methods. Sometimes direct measurements can be made, such as conventional core analysis, image analysis, and mercury injection methods. In other cases indirect measurements may be used, such as geophysical well logs, well test, and artificial neural network methods. Direct measurements are better for understanding the relationship between pore structures and other petrophysical parameters, but they are expensive and time consuming. In image analyses, OM (Optical Microscopy) and SEM (Scanning Electronic Microscopy) petrography are used to characterize key geometric aspects of porosity in each sample. Mercury injection capillary pressure (MICP) as a laboratory method has been used for determining the pore aperture size distribution. Artificial neural network is a new method for permeability determination that is quite inexpensive. It is able to predict the permeability of the formation using the data provided by geophysical well logs. In this case of study that we have only one cored well, prediction of permeability using the same cored well data make errors. Calculating formation porosity from geophysical well loges as an indirect method has been practiced since well logging tools became available.

Methods and Materials

Conventional Core Analysis

Laboratory measurements of the cores attained from the field or core archives, provides precise porosity and permeability values that are used in reservoir simulation studies as well as any other design and development studies on the Field. However porosity and permeability are best measured in the laboratory, but this method has two main limitations 1) Coring is expensive and time consuming with compare to the electronic survey and artificial neural network indirect methods, and 2) It has been a fairly common practice to plot permeability versus porosity for several wells and generate a correlation between these variables for estimating formation permeability in other wells, from which cores are not available. Only for fairly homogeneous reservoirs this effort may or may not prove to be adequate. As the degree of heterogeneity of a reservoir increases such correlation loses credibility. Despite these limitations, both direct and indirect methods have been used in this study, because 1) The cored well is the only available well in the field and can be analyzed using laboratory measurements and 2) Degree of heterogeneity of the reservoir is low. So we have the best measurements of porosity and permeability for determining of rock types and comparison with indirect methods.

The total number of prepared plugs from the core is 109 (83 horizontal plugs, and 26 vertical plugs). Air porosity and helium permeability of all of the plugs were measured using CMS (Core Measurement System)-300 instrument at different net stresses (102 core plugs measured at 800psi net stress and 7 core plugs from different rock types measured at 800, 1500, 2500, 4000 and 5500psi net stresses for consideration of compressibility behavior of the reservoir. Measurements were made on cylindrical plugs, 1.5 inch in diameter and 3 inches in length, drilled from the side of the core.

Image Analysis

A total of 82 thin sections from horizontal plugs of the cored intervals were prepared to characterize their mineralogical components, texture, grain size, pore types, and diagenetic processes of the reservoir. Photomicrographs were taken from all features relevant to reservoir quality. Detailed point count analysis was done to determine the

percentage of intraclasts, the amount and type of pore filling constituents, and the percentage of visible pore spaces. In order to validate the OM petrographical analyses, 8 samples were selected for SEM petrography. SEM images reveal size and geometry of the pores and pore throats clearly.

Pore space analysis using OM images provide macroporosity information, whereas the SEM images yield information on microporosity. OM and SEM petrography are used to characterize key geometric aspects of porosity in each sample. Comparison of total porosity determined from plugs indicates that macroporosity and microporosity values based on image analysis match the plug data, confirming the validity of the method. The combination of macroporosity and microporosity data yields pore size distribution and pore shape information that can explain the distribution of physical properties, in particular permeability. Permeability is mainly controlled by the macropore shape in high-permeability samples, and by the amount of intrinsic microporosity in the low permeability samples.

Geophysical Well Logs

Because, few cores are taken and most wells have wireline logs, the rock fabric information obtained from core description must be calibrated to logs to increase the distribution of data over the reservoir.

Calculating formation porosity from geophysical well logs (sonic, neutron and density logs) has been practiced since well logs became available.

Permeability is a difficult parameter to estimate from wireline logs. There are so many variables controlling the flow of fluids in the reservoir; matrix properties, fractures, sedimentary structures, fluid properties, etc. The relationships between core porosity and core permeability and an artificial neural network have been used for the estimation of a continuous permeability curve separately. In the first method two models have been established, as below:

$$RT: 1,2 \qquad KLOG = 10^{(20.688 \times PHIE - 2.6424)} \qquad R^2 = 0.53$$

$$RT: 3,4 \qquad KLOG = 10^{(7.6629 \times PHIE - 1.0927)} \qquad R^2 = 0.67$$

Different crossplots were drawn to distinguish rock types using log data. Figure 1-A shows core porosity versus core permeability. Figures 1-C and 1-E show logs derived permeability were plotted against log porosity for the two permeability estimation methods separately. In the Figure 1-D water saturation from log is presented in the Z axis of porosity-permeability crossplot.

Artificial neural network is able to predict relatively accurate permeabilities of the formation, using the data provided by core analysis and geophysical well logs. Neural network can be used as a simple tool to confirm results. It is also a powerful predictive method in uncored wells, or distance between consecutive plugs in a cored well. It does not require production interruption and provides permeability values that are comparable to those obtained by laboratory measurements of cores.

Mercury Injection Capillary Pressure (MICP)

Mercury injection as a laboratory method for determining of pore aperture size distribution in porous rocks was first suggested by Washburn (1921). Afterwards, Purcell (1949) was instrumental in developing mercury injection techniques. Capillary pressure versus mercury saturation is commonly plotted on arithmetic or semi-log plots, although the saturation scale is sometimes reversed so that it increases from right to left. The time required for the mercury-injection system to reach equilibrium at each pressure depends on permeability and pore geometry.

The mercury capillary pressure curve after correction for the entry pressure and the volumes normalized by the bulk sample volume is more useful if it can be reduced to a smaller set of parameters that characterized the rock. Clay minerals have main effects on the permeability and capillary pressure curve. The “pore lining” chlorite reduces the permeability. The pore bridging chlorite spans the pore throats and thus greatly increases the capillary pressure and reduces the permeability. Notice that these clays have little effects on the porosity.

In this investigation eight samples from different rock types have been selected for consideration of MICP curves’ behavior and were compared with the results of SEM and thin section micrographs (Figure 2).

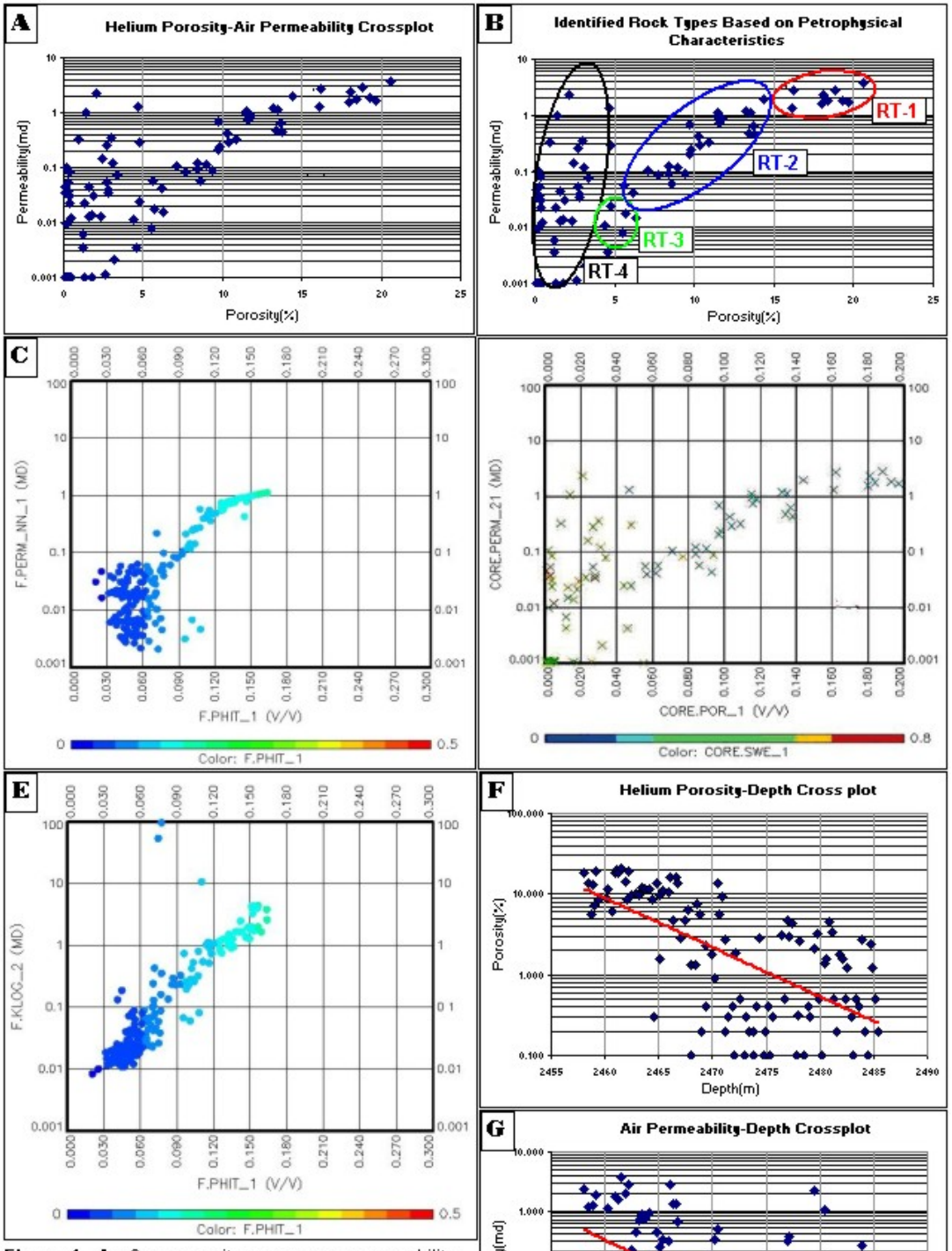

Figure 1– A : Core porosity versus core permeability , **B** : different rock types that identified based on petrophysical parameters,geological and fluid flow characteristics.**C**: Log derived permeability using neural network versus log derived porosity with total porosity in Z axis. **D** : Water saturation from log is presented in the Z axis of por_perm crossplot. ,**E**:Log derived permeability using porosity to permeability transformt log derived porosity with total porosity in Z axis., **F** : Helium porosity versus depth, and **G** : Air permeability versus depth crossplot.

Pore Volume Compressibility

Pore volume compressibility is an important parameter in material balance calculations and reservoir performance studies. Laboratory data show that pore volume compressibility changes along with porosity and permeability variations. That is the type of porosity influences the compressibility and the permeability of rock.

Compact tests using CMS-300 equipment and pore volume compressibility tests were performed on more than 100 core plugs taken from the carbonate reservoir. This formation is mainly a non-vuggy and non-fractured carbonate reservoir rock. The tests have been carried out under several net stresses during increasing and decreasing stress cycles. The samples subject to analysis have been classified into three main groups: 1) The first group indicates a normal and smoothly decreasing trend of compressibility, porosity, and permeability as the applied net stress increases. This group may be considered as the representative of homogenous carbonate rock with interparticle porosity, in which, rising net stress will yield on particle compaction. 2) The second group sharply decreases within the first region (less than 2500 psi) because of decrease in compressibility, porosity, and permeability trends. Until they remain almost constant within the second region (more than 2500 psi). This group has a bimodal type of porosity. 3) The third group is an unusual case. In this group, the curves follow increasing trends instead of decreasing.

Properties obtained from CMS-300, have been used to calculate the pore volume compressibilities and then the pore volumes obtained from it, be used to calculate the pore volume compressibility at each net stress-increasing interval.

Sedimentology and Petrographical Observations

Recognition of relationships between lithofacies and pore size distribution is the basis for petrophysical characterization of the reservoir. Thin section petrography and scanned electron microscope images are used to define mineralogy, rock fabric, texture, diagenetic features and pore size and geometry of the reservoir.

Calcite, either amorphous or crystalline forms the dominant type of mineral. In addition dolomite, clay minerals and opaque mineral fragments are abundant as well. Chalk patches sometimes can be seen

in minor amounts. Grain size ranges from 0.1μm to greater than 500 μm, but most grains are less than 20 μm.

According to the modified Dunham (1962), and Lucia (1995) carbonate classification scheme, the reservoir rock is typically medium to high porosity mud-dominated bioclastic packstone (Oligostegina limestone). The rock fabric displays two forms, massive and pressure welded bituminous fabric.

Sedimentological analysis of the core shows two facies associations: The first is mud dominated bioclastic peloidal packstone, packstone/grainstone and grainstone, partialy dolomitized and cemented with good to fair interparticle porosity, common bioclasts and some opaque minerals (in pyrite and sphalerite). This facies association is indicative for a proximal, open marine depositional environment. The second is mud dominated planctonic foraminiferal packstone/ grainstone (Oligostegina facies), Packstone/wackestone and wackestone. A pressure welded bituminous and generally partially cemented fabric is common. This facies association indicates a distal open marine depositional environment.

Results and Discussion

Porosity and permeability distribution core analysis data

The porosity versus permeability distribution of all 109 plug data displays considerable scatter, even in semi-log plots (Figures 1-A and 1-B), where porosities range from 0.1 to 20.6% and permeability range from 0.001 to 3.776 md, rather than the usual linear relationship between porosity and permeability. Porosity enhancement via matrix dissolution reaches a critical point is a possible explanation for the unusual abundant data points at relatively low porosities paired with low permeabilities (Figure.1-A, RT4). Alternatively the samples combining relatively fair porosity and low permeability (Figure.1-A, RT2) may be explained by saturation with bitumen of the most porous carbonates. Some of this bitumen could not be extracted even after two weeks. The samples with good porosity and low permeability may represent porous carbonate with interparticle and vuggy porosity (Figure.1-A, RT1). About 90% of the total plug data set ranges from 0.1 to 15% porosity and 0.001 to 1 md permeability.

Permeability-Depth relationships in this reservoir (Figure.1-G) have many similarities to the documented porosity depth trends (Figure.1-F). Like the permeability trends, the porosity trends also predict that the rocks with the best reservoir quality in the near surface are most likely the better reservoirs at well intervals. Texture is also critical, because grain-supported limestones behave differently than mud-supported rocks. Matrix permeability is much more sensitive to burial compaction than porosity. Moreover, permeability evolution with burial rather than porosity evolution may be the critical factor in the preservation of reservoir quality in a limestone. This clearly illustrates that the rate of matrix permeability loss with depth is greater than the rate of porosity loss.

Pore space and pore throat textures

Pore spaces between the grains of mud-dominated fabrics are filled with mud even if the grains appear to form a supporting framework. Therefore it is very important to assess the relationships among microcrystalline calcites. The role of microporosity to quantitative reservoir characterization can be a combination of microscopic observations, SEM petrography, and capillary pressure curve characteristics. Pore types of the reservoir can be categorized into interparticle and/or intercrystal microporosity, interparticle dissolution porosity, and primary or solution microporosity in the mud matrix.

Pore systems have been identified on the basis of size, shape, origin and distribution using qualitative thin section, SEM micrographs and physical parameters. Entry pressure measurements (in psi) is indicative of the largest pore size. Minimum unsaturated pore volume is expressed in percent and reflects irreducible residual saturation. Geometric description of the curve or c-factor is a measure of the pore sorting measured by MICPM. Low values indicate good sorting. The petrophysical parameters (pd, Sm and c-factor) adequately describe a curve and provide a good basis for pore system classification and determination of rock types. These procedures reveal that the pore systems of the reservoir consist of varying proportions of three types: primary intergranular pores (Figure.2-A&B), vugs (Figure.2-A-6&14), and intercrystaline pores (Figure.2-C).

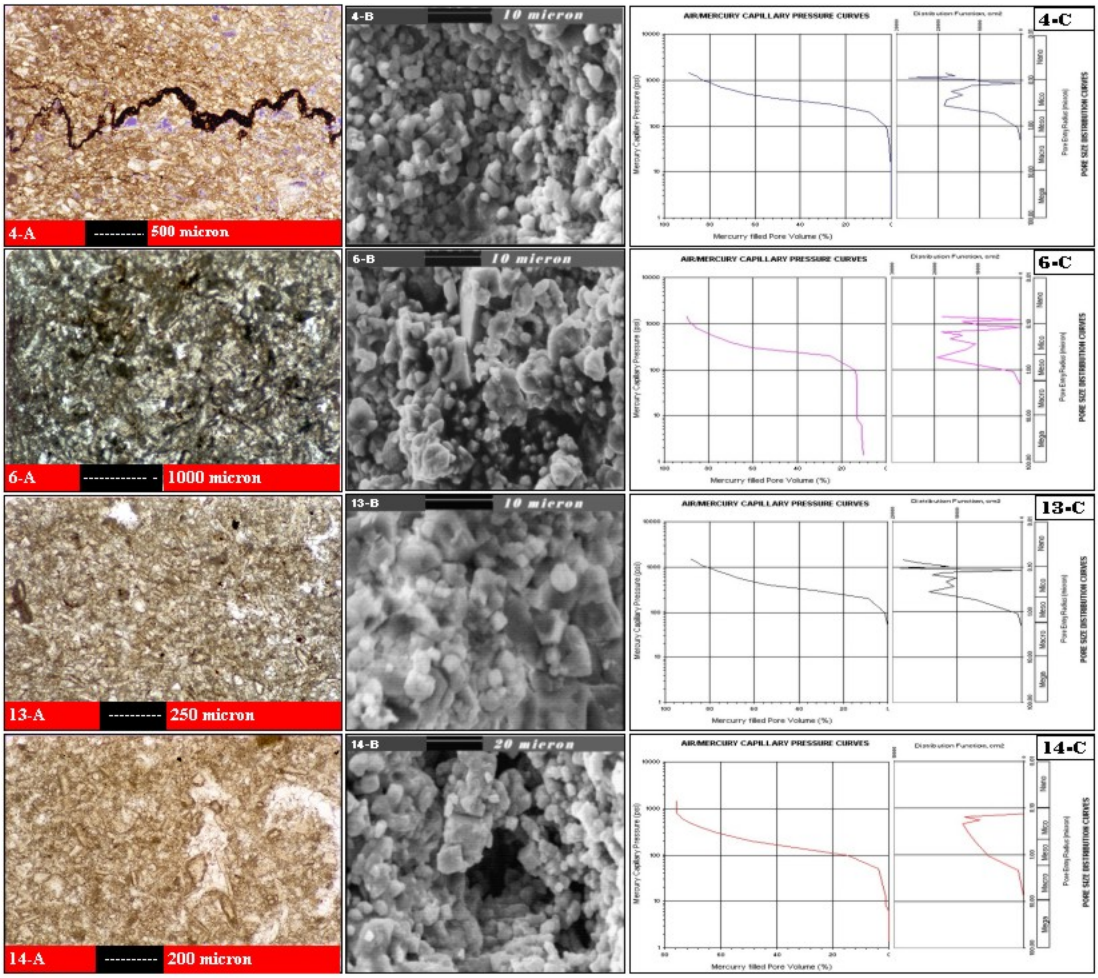

Figure 2-A : Integration of capillary pressure profiles and OM & SEM images for identifing the rock type 1. OM and SEM images show different sizes of grains (less than 5 µm for microcrystaline calcite and more than 5 µm for large crystals and bioclastic particles) and pores (less than 1 µm for nano-pores and more than 1 µm for micro-pores) in the mud dominated bioclastic packstones. Capillary pressure profiles and pore throat size distribution curves show a bimodality of pore geometry ranges from nano to meso.

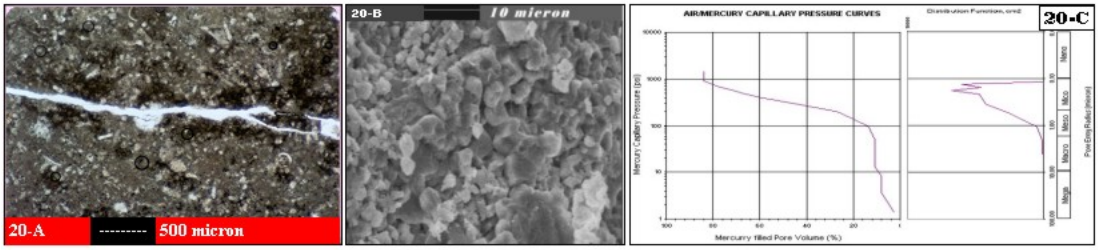

Figure 2-B : Integration of capillary pressure profiles and OM & SEM images for identifing the rock type 2. OM and SEM images show different sizes of grains (less than 5 µm for microcrystaline calcite and more than 5 µm for large crystals and bioclastic particles) and pores (less than 1 µm for nano-pores and more than 1 µm for mezo-pores) in the mud dominated bioclastic packstones. Capillary pressure profiles and pore throat size distribution curves show a unimodality of pore geometry ranges from micro to macro.

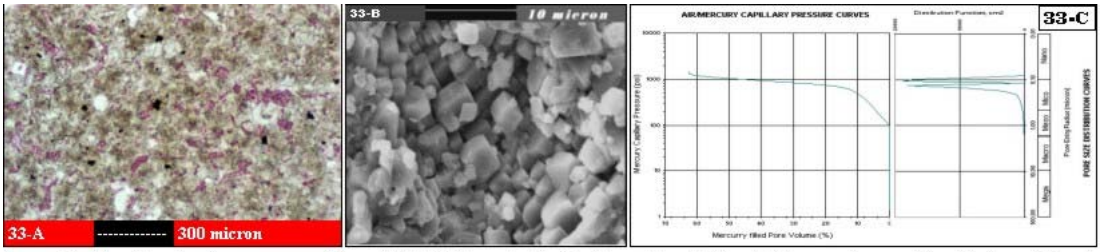

Figure 2-C : Integration of capillary pressure profiles and OM & SEM images for identifing the rock type 3. OM and SEM images show crystaline dolomite and different types of micro-pores. Capillary pressure profiles and pore throat size distribution curves show a unimodality of pore geometry ranges from nano to micro.

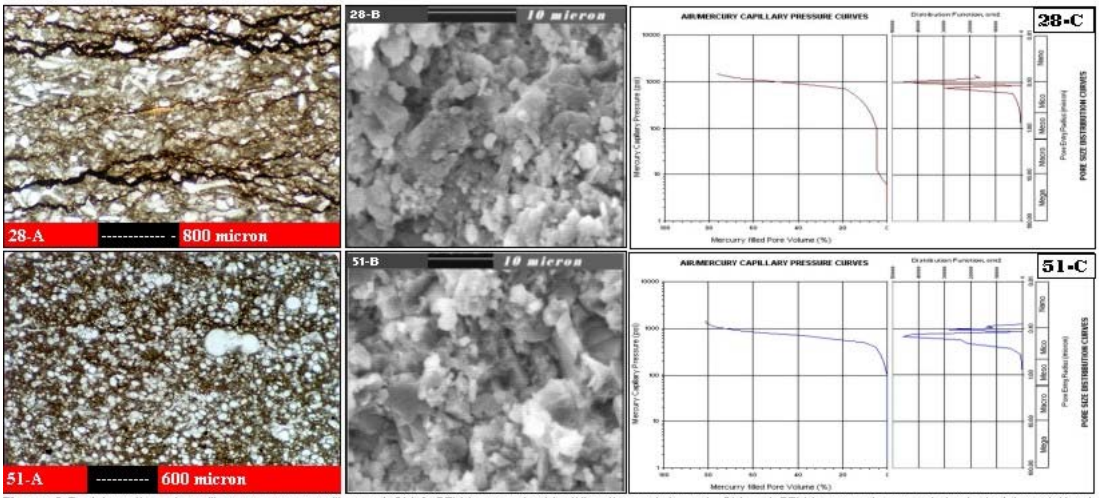

Figure 2-D : Integration of capillary pressure profiles and OM & SEM images for identifing the rock type 4. OM and SEM images show mud dominated foraminiferal packstone with different sizes of grains (less than 5 µm for microcrystaline calcite and more than 5 µm for large crystals and bioclastic particles). Capillary pressure profiles and pore throat size distribution curves show an unimodality of pore geometry range from nano to micro.

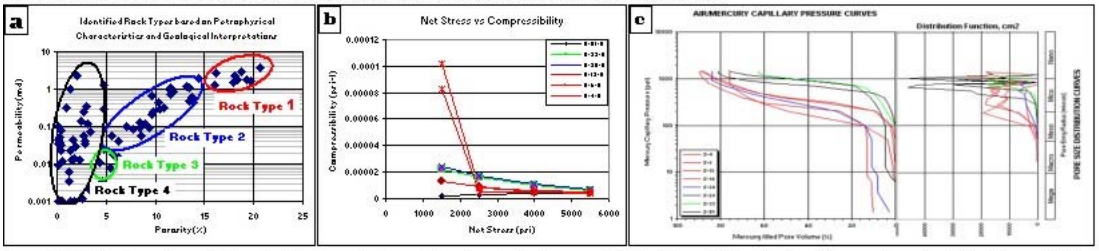

Figure 2-E : This figure shows different rock types using three different methods in comparable togethers. **a**) determined rock types using petrophisical characteristics and geological descriptions., **b**) Compressibility versus net stress that shows three types of rock with different behaviors,and **c**) Capillary pressure profiles and pore throat size distribution curves that show four different categories of rocks.

Pore throat textures involve all void components (pore, pore throat, channel, fracture, etc.) in the rock, and can be categorized into four types based on the geometry and MICPM curves, (Wardlaw and McKellar, 1981). Pore throat textures are useful in characterizing matrix heterogeneity and recovery efficiency.

Pore throat texture A represents homogeneous pore throat and porosity. It corresponds to a symmetric sharp-peaked MICP curve. Pore throat texture B represents a heterogeneous texture of over sized pores tight matrix blocks, and areas of intercrystaline pores. This is comparable with pore throat texture in Figure 2-A (14-A-C). Pore

throat texture C represents a dual-porosity texture of intragranular/ intracrystaline microporosity versus. intergranular /intercrystaline mesoporosity. This type of pore throat texture is common and easily recognizable in the core Figure 2-A (4,6, and 13 A-C). Pore throat texture D is composed of alternating laminations with two sizes of pores, as shown in Figure 2-D (28 and 51-A-C). This type of pore throat texture has bimodal MICPM curve. Individual samples may have bimodal or sometimes polymodal cures, the cumulative injection curves display two corresponding plateaus.

Regarding the pore throat textures, such as those discussed above, generally four aspects of pore systems dominate the trapping of non-wetting phase during withdrawal:

1. Pore shape and pore-to-throat size ratio.
2. Throat-to-pore coordination number.
3. Random and nonrandom heterogeneity.
4. Pore and throat roughness.

Pore shape, pore-to-throat size ratio, and random/nonrandom heterogeneity appear to be the most influential features in most carbonate reservoirs (Luo and Machel, 1995). In samples with the strongest heterogeneity (pore throat textures) large over-sized pores are connected by small intercrystal throats, or the pores are isolated within relatively light blocks, which typically results in low recovery efficiencies.

Combined Rock and Fluid Characteristics

Integration of geological and petrophysical data allows development of a rock–fluid model in the reservoir. Different rock types that comprise the subject reservoirs, marginal reservoirs and non-reservoir rocks are identified in this study. A rock type is defined as an interval of rock with unique pore geometry, determined mineralogical composition and related to specific fluid flow characteristics. The rock fluid model relates to fluid flow characteristics of rock types. Integration of results of the various analytical techniques reveals that the four small-scale lithofacies described using thin section analysis are consistent with the petrophysical model shown in this investigation.

The larger flow capacities in non-reservoir rock types are probably related to higher amounts of clay minerals, affecting the pore throat connectivity and fining the pore throats between microcrystalline calcites in these small-scale lithofacies. The importance of non-depositional factors with regard to reservoir quality, as revealed by core study, indicates a need to define specific rock types on the basis of integrated petrographic, petrophysical, and compositional information. In total, four rock types with individual pore geometries, mineralogy, and fluid flow characteristics were identified in the reservoir.

Rock Type1:

Mineralogy and pore geometry:

Mud dominated bioclastic ploidal packstone, dominantly consisting of calcite minerals. Opaque and clay minerals and dolomitic crystals may be present in subordinate traces.

Porosity is dominantly interparticle and vuggy. Interparticle porosity is essentially represented by two types, one with a large pore volume (pores between bioclastic particles) and the other with relatively small pore volume (micropores, pores between microcrystalline calcite). Vuggy pore spaces are essentially connected. Effective porosity and permeability are fair, despite the fact that the total porosity is good.

Petrophysical characteristics and net pay:

The amount of porosity in rock type 1 varies from 16.1% to 20.6%, with average of 18.4%. Permeability ranges between 1.311md to 3.776md with average of 2.199md. The correlation between permeability and porosity is very poor at best (Figure. 1-B).

Capillary pressure character is uniform, and irreducible water saturations are generally between 10% and 20%. This petrophysical-mineralogical facies has relatively high storage. The pore size distribution is the main control on net pay and ranges meso to nano, whereas pore sorting is medium. Unsaturated pore volume and pore entry pressure are low to medium (table1). These values are mainly a result of good porosity and very fine pore throats. This rock type has low to medium flow capacity and so it acts as a reservoir.

Table 1 - Parameters taken from pc and pore size distribution curves.

Sample No.	Sample depth (m)	Litho-facies	Rock Type (MICPM)	ϕ (%)	K (md)	Pd (psi)	Sm (%)	C
S-4-H	2458.9	MDBPP	Micro-Meso	F	F	L	L	M
S-6-H	2459.2	MDBPP	Nanno-Meso	G	F	L	L	M
S-13-H	2461.2	MDBPP	Nanno-Meso	G	F	M	M	M
S-14-H	2461.5	MDBPP	Meso	G	F	L	H	M
S-20-H	2463.2	MDBPP	Micro-Meso	F	L	L	M	M
S-28-H	2465.1	MDBPP	Nanno-Micro	F	L	VL	H	P
S-33-H	2466.3	Dolostone	Nanno-Micro	L	F	VL	H	M
S-51-H	2470.9	MDFP	Nanno-Micro	F	L	M	M	M

Quality ranges are as follow:

C-factor: Measure of pore sorting
0.1-0.5 Good (G)
0.5-1.0 Medium (M)
>1.0 Poor (P)
K-Air permeability (md)
< 1 Low (L)
1-10 Fair (F)
10-100 Good(G)
>100 Excellent (E)
ϕ–Total Porosity (%)
< 5 Low (L)
5-10 Fair (F)
15-25 Good (G)
> 25 Excellent (E)

Sm-Unsaturated pore volume(%)
< 10 Low (L)
10-20 Medium (M)
>20 High (H)
Pd-Entry pressure (psi)
< 10 Very Low (VL) >24 micron
10-25 Low (L) 24-8 micron
25-100 Medium (M) 8-2 micron
>100 High (H) < 2 micron
RT-Entry pressure (M)
< o.1 None
0.1-0.5 Micro
0.5-2.0 Meso
2.0-10 Macro
> 10 Mega

Mineralogical effect on wireline logs:

According to the mineralogical components, rock type represents a comparatively clean limestone. Presence of minor amounts of clay minerals result in occasional small deflections in the gamma ray logs. In addition, evaporites are absent and dense minerals such as dolomite, occur only in minor quantities. Accordingly, no corrections for sonic, neutron, and density logs are required.

Rock Type 2:

Mineralogy and pore geometry:

Mud dominated bioclastic packstone to bioclastic grainstone, dominantly consisting of calcite minerals (more than 80%), dolomitic crystals (about 15%), and opaque and clay minerals (less than 5%).

Porosity is dominantly interparticle and only occasionally vuggy. Interparticle porosity is essentially represented by two types:

interbioclastic particles with large pores and matrix porosity with very small pores. Vuggy pore spaces are rare and dominantly separated. The total porosity is fair, whereas effective porosity and permeability are fair to low:
Petrophysical characteristics and net pay: Porosity ranges between 5.5% and 14.5%, with average of 9.9%. Permeability is from 0.008md to 1.961md, with an average of 0.446md. The correlation between permeability and porosity is low (Figure. 1-B). Pore sorting is medium and pore size distribution ranges from meso to nano scale. Unsaturated pore volume and pore entry pressures are low (table 1). The petrophysical parameter values show moderate porosity with very fine pore throats. This rock type has low flow capacity and so it acts as a poor reservoir.

Mineralogical effect on wireline logs:
Mineralogically, rock type 2 represents a relatively clean limestone, with minor amounts of clay and crystalline dolomite. Accordingly, deflections in the gamma ray log are small errors in porosity logs because of dolomite are small as well and ignorable.

Rock type 3:
Mineralogy and pore geometry: Rock type 3 contains abundant dolomite, typically as 10 to 100 micrometer euhedral crystals.

Intercrystaline pore space controls the dominant porosity in this rock type. Because the packing of the crystals is very interlocking, the intercrystaline pore spaces are small and pore throats narrow. Although the total porosity is low the permeability is fair, because of good connectivity between the small pores.

Petrophysical characteristics and net pay:
Permeability ranges from 0.039md to 1.302 md, with a mean typically about 0.671md. Porosity varies from 2.8% to 4.7%, with an average 3.75%. For a given porosity value, permeability is greater in this rock type than in the others. The pore sorting is medium and pore size distribution is in ranges from nano to micro scale. Unsaturated pore volume is high and pore entry pressure is very low (table1). This

petrophysical-mineralogical facies has relatively low storage and low to moderate flow capacity.

Mineralogical effect on petrophysical wireline logs:
Because of very little clay content, the deflection curve of the gamma ray log is low and it shows good correlation with core descriptions .

Rock Type 4:

Mineralogy and pore geometry:
Rock type 4 consists of mud dominated pelagic foraminiferous packstone. Calcite minerals are about 80%, clay minerals less than 15%, and dolomitic crystals about 15%.

Matrix porosity is dominantly consisting of connected microcropore spaces, and vuggy porosity is rare in this rock type. However both the total porosity and permeability are low.

Petrophysical characteristics and net pay:
The porosity ranges between 0.1% to 4.8%, with an average of 1.3%. Permeability is between 0.001md to 1.302md with an average of 0.106md. The correlation between permeability and porosity is low and it shows some unusual points with fair permeability and low porosity because of some fractures (Figure. 1-B). The pore sorting is medium and pore size distribution ranges from nano to micro scale. Unsaturated pore volume and pore entry pressure are medium (table1). The petrophysical parameter values point at low porosity with very fine pore throats associating with the low flow capacity non-reservoir.

Mineralogical effect on wireline logs:
The presence of about 15% clay minerals in the carbonate mud of rock type 4 has different effects on geophysical well logs. The clays present in the reservoir reduce the reservoir pore space and fluid conductivity, by forming pore lining, pore coating, and pore filling. In rocks containing clay all porosity logs overestimate porosity. Acoustic and density logs are most affected by clay, having a positive 2% error when clay volume is 10%. Neutron logs are less affected by clay, having less than 1% error at 10% bulk volume clay. The mineralogy indicates that rock type 4 is a limestone, relatively contaminated with

clay minerals. Accordingly, gamma ray logs may be deflected and porosity logs could be erroneous.

Conclusions

- Rock type characterization based on different petrophysical parameters, geophysical well logs and geological studies show the same results. So, geophysical well logs and petrophysical parameters allow classification of the reservoir into petrophysical flow units without calibration by cores.
- Pore system heterogeneity may be easily characterized not only by using the SEM micrographs and the pore size distribution curves, but also concluded from the compressibility curves. Compressibility investigations in this study indicate that there is a good comparison between compressibility trends and the identified rock types.
- The mercury injection capillary pressure and pore size distribution curves indicate some heterogeneity at the top and homogeneity in the middle and bottom parts of the reservoir.
- Permeability and porosity-depth relationships in this reservoir have many similarities. Like the permeability trends, the porosity trends predict that the rocks have better reservoir quality in the near surface is most likely the better reservoirs at the middle and bottom. This clearly illustrates that the rate of matrix permeability loss with depth is greater than the rate of porosity loss.

Acknowledgments

The author thanks the Core Analysis Department of RIPI, specially Mr. E. Kazemzadeh, A. Sadegh-Azad and H. Bakhtiari for preparing of the conventional and core analysis data and Anton Koopman for editing the paper.

References

Aiassa, D.A., Di Renzo, M.A., and Ibáñez, M.A. (1995) *Estimación de la diversidad isoenzimática de dos especies de Bromus*. Turrialba, **45**, 1-7.

Altube, H.A., Cabello, F., and Ortiz, J.M. (1992) *Caracterización de variedades y portainjertos de vid (Vitis vinifera L.) mediante isoenzimas de las raices*. Agriscientia **9**, 21-29.

Baudoin, J.P. (1991) *La culture el l'amélioration de la légumineuse alimentaire Phaseolus lunatus L. en zones tropicale*. Ede, Pays-Bas: CTA.

Boulter, D., and Thurman, D. (1968) *Acrylamide gel electrophoresis of proteins in plant systematics. In J.G. Hawkes (ed.), Chemotaxonomy and Serotaxonomy*. Academic Press. London, pp. 39-48

Bravi, R., Sommovigo, A., Delogu, C., and Merisio, G. (1994) *Indagine sullidentita specifica del seme di Lolium rigidum commercializzato in Italia*. Sementi Selette **40**, 1-17.

Bressani, R., and Elias, L.G. (1980) *Nutritional value of legume crops for humans and animals*. In R.J. Summerfield and A.H. Bunting (eds.), Advances in legume science. Kew, Richmond, London: Royal Botanical Gardens, p. 135-155.

Carreras, M.E., Fuentes, E., and Merino, E.F. (1997) *Seed protein patterns of nine species of Cactaceae.* Biochem.Syst.Ecol. **25**, 43-49.

Duvall, M.R., and Biesboer, D.D. (1989) *Comparisons of electrophoretic seed protein profiles among North American populations of Zizania*. Biochem. Syst. Ecol. **17**, 39-43.

Jansman, A.J.M. (1996) *Bioavailability of proteins in legume seeds.* Grain Legumes (AEP) **11**, p.429-432.

Johnson, B.L., Barnhart, D., and Hall, O. (1967) *Analysis of genome and species relationships in the polyploid wheats by protein electrophoresis*. Am. J. Bot. **54**, 1089-1098.

Harborne, J.B., and Turner, B. (1984) *Plant biosystematics*. London.

Laemmeli, U.K. (1970) *Cleavage of structural proteins during the assembly of the head of bacteriophage T4*. Nature **222**, 680-685.

Leconte, A., Lebrun, P., Nicolas, D., and Segiun, M. (1994) *Electrophoréses application á I′identification clonale de I′ hevea.* Plantations recherche development, **1**, 28-33.

Mahe, S., Gausseres, N., and Tome, D. (1994) *Legume proteins for human requirements*. Grain Legume (AEP) **7,** 15-17.

Makai, S., and Balatincz, J. (1998) *Study of seed protein content of fenugreek (Trigonella foenum-graecum L.)*. Man-Agriculture-Health, p.167-171

Misset, M.T., and Fontenelle, C. (1992) *Protein relationships between natural populations of Ulex europaeus and U. galli (Faboideae, Genisteae) and their hybrids*. Pl. Syst. Evol. **179**, 19-25.

Norton, G., Bliss, F.A., and Bressani, R. (1985) *Biochemical and nutritional attributes of grain legumes. In R.J. Summmmerfield and E.H. Roberts* (eds.), Grain legume crops. London: Collins, p.73-114.

Otoul, E. (1976) *Spectres des acides aminés chez Phaseolus lunantus L., chez quelques espéces apparentées et chez l'amphidiploïde P. lunatus L.x P.polystachyus(L.) B.S. et P. Bull*. Rech. Agron. Gembloux, **11**, p.207-220.

Pascale, N.C., Camdessus, M.C., and Lenardis, A.E. (1994) *Diferenciacion de cultivares de soja (Glycin max L.). Merill) por técnicas de laboratorio*. Oleaginosos **7**, 12-16.

Pasha, M.K., and Sen, S.P. (1991) *Seed protein pattern of Cucurbitaceae and their taxonomic implications.* Biochem. Syst. Ecol. **19**, 569-576.

Patil, S.P., Niphadkar, P.V., and Bapat, M.M. (1997) *Allergy to fenugreek (Trigonella foenum-graecum).* Annals of Allergy, Asthma & Immunology, **78**, 297-300.

Vaughan, J.B. (1983) *The use of seed proteins in taxonomy and phylogeny*. In J. Daussant, J. Mosse and J.B. Vaughan (eds.), Seed proteins. London, pp. 135-153.